Nano World Journal

https://doi.org/10.17756/nwj.2023-s2-051

Research Article

Open Access

Dynamic Thermal Characteristics of Compacted Bentonite Material

Mohamed Essaleh[1*], Rachid Bouferra[1], Soufiane Belhouideg[2], Mohammed Mansori[3] and Abdeltif Bouchehma[2]

[1]L3G Laboratory, FST, Cadi Ayad University, B.P.549, Marrakech, Morocco

[2]RLPES, FP, Sultan Moulay Slimane University, Béni Mellal, Morocco

[3]IMED-Lab, FST, Cadi Ayad University, B.P.549, Marrakech, Morocco

[*]Correspondence to:
Mohamed Essaleh
L3G Laboratory, FST,
Cadi Ayad University,
B.P.549, Marrakech, Morocco.
E-mail: moh.essaleh@gmail.com

Received: July 25, 2023
Accepted: September 26, 2023
Published: September 28, 2023

Citation: Essaleh M, Bouferra R, Belhouideg S, Mansori M, Bouchehma A. 2023. Dynamic Thermal Characteristics of Compacted Bentonite Material. *Nano World J* 9(S2): S300-S304.

Published by United Scientific Group

Abstract

Powder bentonite was analyzed by different experimental techniques. The data from SEM (Scanning electron microscope), XRD (X-ray diffraction), and XRF (X-ray fluorescence) show that bentonite is Na-type, with montmorillonite as the dominant phase. The geotechnical study shows a very plastic silty (I_P = 445 % > 50%) material. The methylene blue value (MBV) is determined to be 0.40 indicating that our bentonite is classified as a sandy silty clay, sensitive to water and not very calcareous. The needed data for the calculations of the dynamic thermal characteristics of compacted bentonite are the thickness of the material, bulk density, thermal conductivity, massic heat capacity, and the period of thermal variations. The thermal conductivity (from 0.3275 W/m.K to 0.4456 W/m.K) as the bulk density (from 2.074 g/cm^3 to 2.292 g/cm^3) of pure bentonite increases with the increase of the compaction intensity (from 10 to 50 bar). The period is one day (86400 s), corresponding to the daily climatic variations. The calculations were made using a flow chart and taking into account the exterior and interior superficial thermal resistances. To improve the thermal and mechanical strength of bentonite, three compositions of sand, cement and lime based on bentonite were used. The composition $B_{15}S_{80}C_5$ with 15% bentonite, 5% cement and 80% sand is the most suitable for eventual use in the building sector since it has a lower damping coefficient and a higher internal capacity.

Keywords

Compacted bentonite, Compressive strength, Thermal conductivity, Heat capacity, Thermal insulation

Introduction

It has been observed that in sand-bentonite mixtures, bentonite which is evenly distributed and fills the voids around sand particles can play the same role as cement in terms of compressive and thermal behaviors [1, 2]. Bentonite is a plastic clay consisting essentially of montmorillonite [3-7] which is an aluminum silicate in laminar structure that contains many charged elements and crystal water [6, 7]. It is widely used in many industrial sectors (pharmaceuticals, cosmetics, chemicals, civil engineering, food industry, etc.) [4, 5, 8].

Heat capacity and thermal conductivity are the main parameters related to how heat is transported through clay materials. It is a question of proving the thermal qualities of these materials, as well as developing new products by incorporating additives in the basic mixture, in order to reduce the thermal conductivity while keeping the mechanical and hydric properties within the standards.

The amount of bentonite and water has a significant influence on compaction, quality, and thermal resistivity [2, 9]. Previous studies on bentonite-cement-sand mixtures have been performed [10-12]. However, less attention has been paid to the study of the effect of compaction intensity and water content on their thermal and mechanical properties. Also, there are no detailed published works on the dynamic thermal characteristics that describe the thermal behavior of bentonite-based building materials [10, 11].

Hence, the purpose of this work is to study the mechanical and thermal properties of compacted pure Moroccan bentonite as well as a dry-mixed sand-bentonite-cement-lime mixture and to investigate the suitability of such mixtures for eventual use in the building and/or environmental sectors. Local raw materials of bentonite, cement, sand, and lime were used in this work. Several analytical techniques: XRD, XRF, and SEM were used in the characterization of materials.

The needed data for the thermal calculations are the thickness of the material, bulk density, thermal conductivity, heat capacity, and the period of thermal variations. The period is one day (86400 s), corresponding to the daily climatic variations. The calculations are made using a flow chart and taking into account the exterior and interior superficial thermal resistances.

Materials and Method

Bentonite material

Pure commercial Moroccan powder bentonite, cement, and lime clays were used in the present study (Figure 1a), with sand from the region of Agadir (Oued Issen) in the south of Morocco. The samples in cylindrical forms (Figure 1b) were prepared for thermal and mechanical measurements. The nominal resistance (R_c) was determined in simple compression with a speed of 0.5 mm/min until rupture (Figure 1c). The thermal conductivity (λ) was measured by considering the Lee's disks device [13-15]. The specific heat capacity (C_p) of bentonite is determined by the mixture method, where heat exchange between the hot solid (compacted bentonite), water, and calorimeter results in all bodies attaining the same final steady temperature (θ_f) after some time. Bentonite materials are nanoscale materials.

Structural and morphological properties

Table 1 presents the XRF chemical composition of bentonite, with the main element SiO_2 (53.50%), mainly from quartz. The Al_2O_3/SiO_2 composition ratio is in the order of 0.32, very close to the suggested theoretical value of 1/3 for montmorillonite. Bentonite is of the sodium type since the content of Na_2O is large compared to that of CaO [16, 17]. Dominant montmorillonite (M) peaks were identified in agreement with the literature [17, 18], and mineral impurities such as quartz and feldspars were also found (Figure 2a). The morphological structure of bentonite was determined by the SEM (TESCAN VEGA$_3$), which shows a porous crystalline structure (Figure 2b).

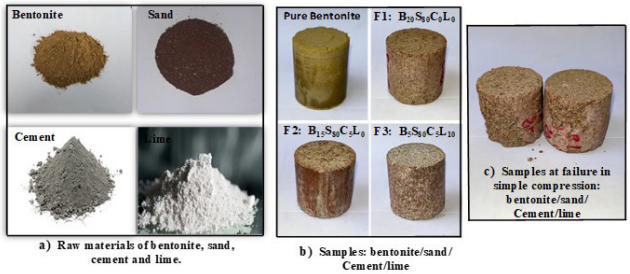

Figure 1: Raw materials of bentonite, sand, cement, and lime **(a)**, samples **(b)** and samples at failure in simple compression **(c)**.

Table 1: Chemical characteristics of bentonite by XRF.

Chemical composition (%)								
SiO_2	Al_2O_3	Fe_2O_3	MgO	CaO	Na_2O	K_2O	TiO_2	MnO
53.50	17.22	8.97	2.60	1.37	3.4	1.2	1.32	0.03

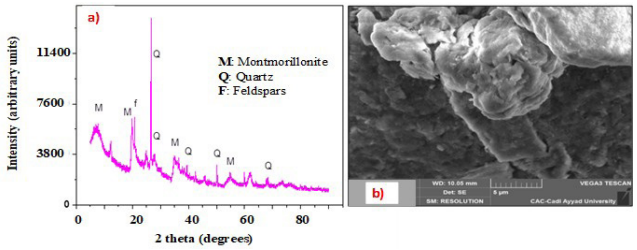

Figure 2: (a) XRD and **(b)** SEM of powder bentonite.

Results and Discussion

Geotechnical characterization

The particle size data of our bentonite indicates, with the European standard [NF EN ISO14688-1, 2003], a clay fraction (9.56%), fine silt (48.44%), medium silt (40.05%), coarse silt (1.95%), and 0% of sand. The Atterberg limits as well as the plasticity (I_P), liquidity (I_L), and consistency (I_C) index of bentonite are estimated. Bentonite is a very plastic clay (I_P = 445% > 50%) with a high-water content (W = 10.5%). The MBV is determined to be 0.40, indicating that our bentonite is classified as a sandy silty clay that is sensitive to water.

Mechanical and thermal analysis

The bulk density, the Young's Module, and the maximum compressive stress of bentonite are given in table 2 for the compaction intensities of 10 bar, 30 bar, and 50 bar (Figure 3a).

With a density varying between 2.074 g/cm^3 and 2.292 g/cm^3, the maximum compressive stress R_c varies between 5.01 MPa and 20.8 MPa, respectively. Furthermore, the massic heat

Table 2: Thermal and mechanical parameters of bentonite.

Compaction intensity (bar)	10	20	30
Bulk density (g/cm^3)	2.074	2.263	2.292
Thermal conductivity (W/m.K)	0.3275	0.3948	0.4456
Young's module (MPa)	272	852	1385
Maximum compressive stress (MPa)	5.01	18.6	20.8
Massic heat capacity (J/Kg.K)	1529	1560	1598
Volumetric heat capacity (MJ/m^3.K)	3.17	3.53	3.66

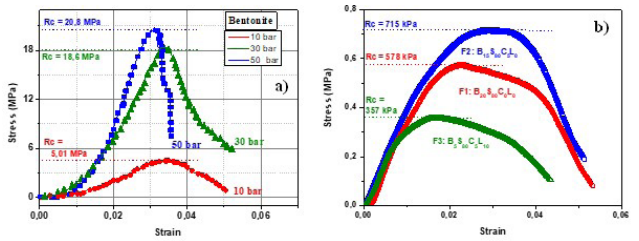

Figure 3: Variation of compressive strength for **(a)** compacted bentonite and **(b)** non-compacted bentonite/sand/cement/lime mixtures.

capacity *C* and the thermal conductivity λ are the significant parameters describing the thermal properties of any material. In addition to the composition and orientation of the minerals in the sample, the bulk density, the porosity, and the water content have a large influence on λ and *C*. The thermal conductivity of bentonite was determined following the two metallic disks device [13-15].

To heat the upper disk, we can use either steam (water vapor) or an electronic regulator through a heating filament. The electronic control has been adopted in our case to maintain the upper disk (A) at T_1 = 80 °C. After some time, the second disk (B) will be in a steady thermal state at T_2 = 54.2 °C, 57.9 °C, and 57.4 °C for the three samples compacted at 10 bar, 30 bar, and 50 bar, respectively. The corresponding thermal conductivity is calculated by using the expression.

$$\lambda\left(\frac{W}{m.K}\right)=\frac{m.C.d.(r+2h).\left[\frac{dT}{dt}\right]_2}{\pi.r^2.(T1-T2).(2r+2h)} \quad (1)$$

Where *m* is the mass, *C* is the massic heat capacity, *r* is the radius, and *h* is the thickness of the lower disc (B). The thickness of the sample is *d*. The rate of cooling of the lower disc (B) at steady state T_2 is represented by the term $\left[\frac{dT}{dt}\right]_{T2}$. The values of $\left[\frac{dT}{dt}\right]_{T2}$ are determined from the first derivative of $T_2(t)$ for the three previous samples of compacted bentonite. The corresponding values of λ are given in table 2, which varies between 0.3275 W/m.K and 0.4456 W/m.K for the samples compacted at 10 bar and 50 bar, respectively. The thermal conductivity as the bulk density increases with the increase in compaction intensity.

As mentioned above, the specific heat capacity of bentonite is determined by the mixture method. Since bentonite reacts strongly with water, the compacted sample is placed inside a copper metal enclosure. The corresponding values of *C* are also given in table 2, which vary between (1529 J/Kg.K or 3.17 MJ/m³K) and (1598 J/Kg.K or 3.66 MJ/m³K) for the samples compacted at 10 bar to 50 bar, respectively. By using the obtained values of λ and *C* for each sample, we are able to analyze the dynamic thermal characteristics describing the thermal behavior of bentonite according to the standard [NF EN ISO 13786, 2008] when it is subjected to variable boundary conditions and its faces are assumed to be subjected to sinusoidally varying temperatures or heat flux. The heat transfer matrix (Z) that relates the temperatures and heat flux densities of the two faces of the material [19] is determined. The quantities used to characterize the dynamic behavior of our samples are (a) the internal surface thermal capacity (C_i), which is the capacity of the internal face of a wall to absorb, store, and restore calories. It characterizes the interior thermal inertia, and (b) The damping factor (f) which is the ratio between the amplitude of the temperature at position x in the wall and that of the exciting temperature. Table 3 summarizes the different thermo-physical properties of the three compacted bentonite samples when considering a typical value of the wall thickness of 0.3 m.

Table 3: Thermophysical properties of the three compacted bentonite samples (Wall thickness = 0.3 m).

Compaction intensity (bar)	10	20	30
Bulk density, ρ (g/cm³)	2.074	2.263	2.292
Thermal conductivity, λ (W/m.K)	0.3275	0.3948	0.4456
Massic heat capacity, C (J/Kg.K)	1529	1560	1598
Damping factor, f	0.02712	0.02979	0.0340
Internal surface thermal capacity, Ci (kJ/m²K)	60.40	64.45	66.60
Thermal resistance, R (m²K/W)	1.086	0.9299	0.8433

The walls of pure bentonite of the highest value of thickness do not allow the building to have thermal insulation. The thermal resistance shows a linear behavior versus the thickness of the wall (Not shown here) is always lower than the required values by the thermal regulations. The use of a wall with pure bentonite requires the use of additional components to reach the highest values of thermal resistance. The internal surface thermal capacity C_i increases quasi-linearly with the thickness of the wall, until reaching its maximum value in the order of 10.73 cm, 11.15 cm, and 11.57 cm for the three cases of 10 bar, 30 bar, and 50 bar, respectively. It is useless from the point of view of thermal capacity to have a thickness higher than these values. Indeed, after the maximum, the capacity decreases asymptotically until reaching a limit value [20]. Concerning the damping factor *f*, this parameter decreases with the increase of the wall thickness, until it reaches a value close to zero. This means that the thickness of the wall attenuates the fluctuations of the external thermal wave, and subsequently, the interior temperature is practically stable and constant. In summary, we can see that the effect of the compaction intensity (from 10 bar to 50 bar) is to increase *f* and C_i, and decrease the thermal resistance *R*.

Finally, in order to improve the mechanical and thermal properties for an eventual use of bentonite in the building sector, we consider, as an initial step, three compositions (F1: $B_{20}S_{80}C_0L_0$), (F2: $B_{15}S_{80}C_5L_0$), and (F3: $B_5S_{80}C_5L_{10}$) of non-compacted and non-sintered sand (S), cement (C), and lime (L) based on bentonite (B). The thermal conductivity decreases when going from F1 to F3, in relation to the increase in porosity caused by the addition of lime and cement to the bentonite-sand mixture. Substituting bentonite with cement has the effect of increasing the compressive strength (F1 to F2), while lime plays the opposite role (F2 to F3) (See figure 3b). Table 4 summarizes the different thermo-physical properties of the three non-compacted and non-sintered compositions F1, F2, and F3. Figure 4a, 4b, and 4c shows the variations of the thermal resistance, the interior surface thermal capacity

(C_i), and the damping factor (f) as a function of the wall thickness of the three non-compacted and non-sintered compositions. The composition F2 is the most suitable for eventual use in the building sector since it has a lower damping coefficient and a higher internal capacity.

For the evolution of the phase shift, the results show that the ideal thickness, to reach the day/night phase shift required for thermal comfort, is between 15.3 cm and 18.5 cm for the bentonite compacted from 10 bar to 50 bar (Figure 5a), and between 32 cm and 39 cm for the composition

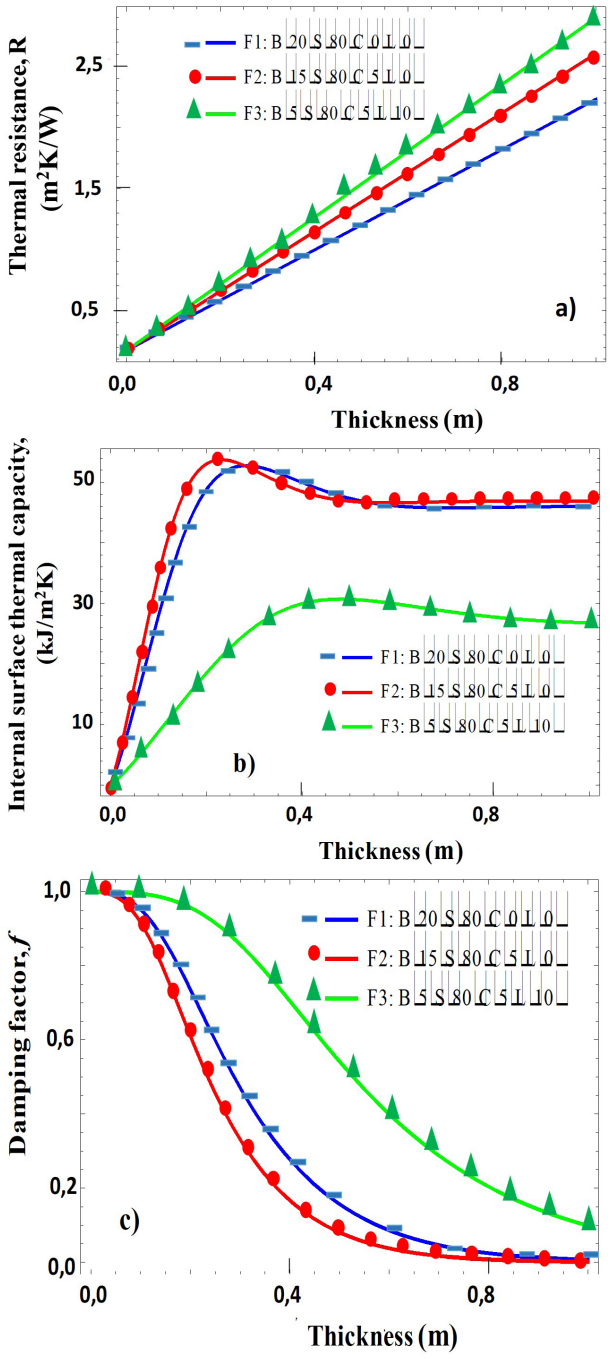

Figure 4: (a) The thermal resistance, **(b)** the internal surface thermal capacity (C_i), and **(c)** the damping factor (f) as a function of the wall thickness of the three non-compacted and non-sintered compositions (F1: $B_{20}S_{80}C_0L_0$), (F2: $B_{15}S_{80}C_5L_0$), and (F3: $B_5S_{80}C_5L_{10}$).

Table 4: Thermophysical properties of the three non-compacted and non-sintered compositions (F1: $B_{20}S_{80}C_0L_0$), (F2: $B_{15}S_{80}C_5L_0$), and (F3: $B_5S_{80}C_5L_{10}$) (Wall thickness, d = 0.3 m).

Sample	F1	F2	F3
Bulk density, ρ (g/cm³)	1.538	1.509	1.398
Thermal conductivity, λ (W/m.K)	0.4853	0.4107	0.3666
Massic heat capacity, C (J/Kg.K)	498.63	638.36	157.36
Damping factor, f	0.4711	0.3314	0.8572
Internal surface thermal capacity, Ci (kJ/m²K)	52.74	51.81	26.00
Thermal resistance, R (m²K/W)	0.7793	0.8941	0.9802

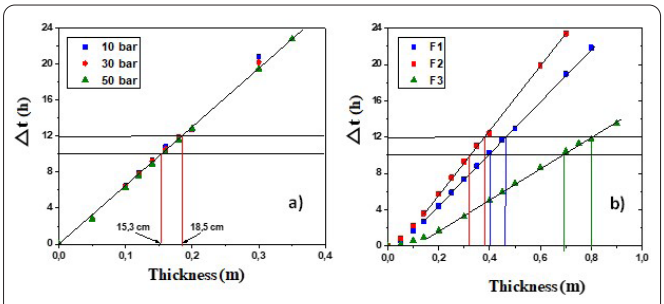

Figure 5: The phase shift as a function of the thickness of the wall of **(a)** compacted bentonite and **(b)** non-compacted compositions (F1: $B_{20}S_{80}C_0L_0$), (F2: $B_{15}S_{80}C_5L_0$), and (F3: $B_5S_{80}C_5L_{10}$).

(F2: $B_{15}S_{80}C_5L_0$) (Figure 5b). However, further similar studies for different compacted bentonite/sand/cement mixtures are needed in order to determine the optimum composition with optimal thermal and mechanical properties.

Conclusion

Na-type pure Moroccan powder bentonite was analyzed by different experimental techniques. The bulk density varies between 2.074 g/cm³ and 2.292 g/cm³ when the compacting intensity varies from 10 to 50 bar. Dynamic thermal characteristics describing the thermal behavior of bentonite according to the standard [NF EN ISO 13786, 2008] are studied. The effect of the compaction intensity is to increase both the damping factor f and the interior surface thermal capacity C_i, and to decrease the thermal resistance R. We present here some initial results on the thermal characteristics of the non-compacted bentonite/sand/cement/lime mixture, showing that the composition F2 ($B_{15}S_{80}C_5L_0$) is the most suitable for eventual use in the building sector since it has a lower damping coefficient and a higher internal capacity. However, further similar studies for different compacted bentonite/sand/cement mixtures are needed in order to determine an optimum composition.

Acknowledgements

None.

Conflict of Interest

On behalf of all authors, the corresponding authors states that there is no conflict of interest.

References

1. Kenney TC, Veen WV, Swallow MA, Sungaila MA. 1992. Hydraulic conductivity of compacted bentonite–sand mixtures. *Can Geotech J* 29(3): 364-374. https://doi.org/10.1139/t92-042
2. Liu M, Hu Y, Lai Z, Yan T, He X, et al. 2020. Influence of various bentonites on the mechanical properties and impermeability of cement mortars. *Constr Build Mater* 241: 118015. https://doi.org/10.1016/j.conbuildmat.2020.118015
3. Rakić V, Rajić N, Daković A, Auroux A. 2013. The adsorption of salicylic acid, acetylsalicylic acid and atenolol from aqueous solutions onto natural zeolites and clays: clinoptilolite, bentonite and kaolin. *Microporous Mesoporous Mater* 166: 185-194. https://doi.org/10.1016/j.micromeso.2012.04.049
4. Sahu M, Reddy VRM, Park C, Sharma P. 2021. Review article on the lattice defect and interface loss mechanisms in kesterite materials and their impact on solar cell performance. *Sol Energy* 230: 13-58. https://doi.org/10.1016/j.solener.2021.10.005
5. Nugroho HS, Refantero G, Septiani NLW, Iqbal M, Marno S, et al. 2022. A progress review on the modification of CZTS(e)-based thin-film solar cells. *J Ind Eng Chem* 105: 83-110. https://doi.org/10.1016/j.jiec.2021.09.010
6. Dlamini MC, Maubane-Nkadimeng, MS, Moma JA. 2021. The use of TiO_2/clay heterostructures in the photocatalytic remediation of water containing organic pollutants: a review. *J Environ Chem Eng* 9(6): 106546. https://doi.org/10.1016/j.jece.2021.106546
7. El-Naggar ME, Wassel AR, Shoueir K. 2021. Visible-light driven photocatalytic effectiveness for solid-state synthesis of ZnO/natural clay/TiO_2 nanoarchitectures towards complete decolorization of methylene blue from aqueous solution. *Environ Nanotechnol Monit Manag* 15: 100425. https://doi.org/10.1016/j.enmm.2020.100425
8. Sedaghat ME, Booshehri MR, Nazarifar MR, Farhadi F. 2014. Surfactant modified bentonite (CTMAB-bentonite) as a solid heterogeneous catalyst for the rapid synthesis of 3, 4-dihydropyrano [c] chromene derivatives. *Appl Clay Sci* 95: 55-59. https://doi.org/10.1016/j.clay.2014.02.016
9. Devrim A, Esener BA. 2011. Usability of sand-bentonite-cement mixture in the construction of unpermeable layer. *Sci Res Essays* 6(21): 4492-4503. https://doi.org/10.5897/SRE10.1189
10. Cheng H, Li W, Chen R, Yi Y. 2022. Workability study of sand-bentonite-cement mixtures for construction of two-phase cut-off wall. *Constr Build Mater* 345: 128058. https://doi.org/10.1016/j.conbuildmat.2022.128058
11. Hashemi MA, Massart TJ, Salager S, Herrier G, François B. 2015. Pore scale characterization of lime-treated sand–bentonite mixtures. *Appl Clay Sci* 111: 50-60. https://doi.org/10.1016/j.clay.2015.04.001
12. Devarangadi M, Shankar MU. 2021. Effect on engineering properties of ground granulated blast furnace slag admixed with laterite soil, cement and bentonite mixtures as a liner in landfill. *J Clean Prod* 329: 129757. https://doi.org/10.1016/j.jclepro.2021.129757
13. Hein A, Müller NS, Day PM, Kilikoglou V. 2008. Thermal conductivity of archaeological ceramics: the effect of inclusions, porosity and firing temperature. *Thermochim Acta* 480(1-2): 35-42. https://doi.org/10.1016/j.tca.2008.09.012
14. Randazzo L, Montana G, Hein A, Castiglia A, Rodonò G, et al. 2016. Moisture absorption, thermal conductivity and noise mitigation of clay based plasters: the influence of mineralogical and textural characteristics. *Appl Clay Sci* 132: 498-507. https://doi.org/10.1016/j.clay.2016.07.021
15. Hein A, Karatasios I, Müller NS, Kilikoglou V. 2013. Heat transfer properties of pyrotechnical ceramics used in ancient metallurgy. *Thermochim Acta* 573: 87-94. https://doi.org/10.1016/j.tca.2013.09.024
16. Veblen DR, Guthrie GD, Livi KJ, Reynolds RC. 1990. High-resolution transmission electron microscopy and electron diffraction of mixed-layer illite/smectite: experimental results. *Clays Clay Miner* 38: 1-13. https://doi.org/10.1346/CCMN.1990.0380101
17. Zaher AMS, Wahab ASM, Taha MH, Masoud AM. 2018. Sorption characteristics of iron, fluoride and phosphate from wastewater of phosphate fertilizer plant using natural sodium bentonite. *J Membr Sci Technol* 8: 1-10.
18. Kumar A, Lingfa P. 2020. Sodium bentonite and kaolin clays: comparative study on their FT-IR, XRF, and XRD. *Mater Today Proc* 22: 737-742. https://doi.org/10.1016/j.matpr.2019.10.037
19. Maillet D, Andre S, Batsale JC, Degiovanni A, Moyne C. 2000. Thermal Quadrupoles. John Wiley & Sons, New York.
20. Sambou V. 2008. Unsteady heat transfers: towards an optimization of building walls. Paul Sabatier University. (Doctoral Dissertation)